MOLECULAR PHYSICS REPORTS **40** (2004) 119-124

TUNING OF ULTRATHIN COBALT FILM MAGNETIC PROPERTIES BY UNDERLAYER AND OVERLAYER STRUCTURES

A. MAZIEWSKI[1], M. KISIELEWSKI[1], Z. KURANT[2], M. TEKIELAK[1], A. WAWRO[2], AND L. T. BACZEWSKI[2]

[1]*Institute of Experimental Physics, University of Białystok*
Lipowa 41, 15-424 Bialystok, Poland

[2]*Institute of Physics Polish Academy of Sciences*
Aleja Lotników 32/46, 02-668 Warsaw, Poland

Abstract: The samples were grown in a molecular beam epitaxy system on sapphire substrate in the following order: (i) Mo buffer; (ii) gold wedge; (iii) ultrathin cobalt wedge; (iv) a metal X (Ag, Cr, Mo) wedge perpendicular to the Co one; (v) Au coverage. Magnetic anisotropy and the coercivity field were studied as a function of both cobalt thickness *d* and metal X thickness *h*. The cover layer of a few monolayers of X has been found to have a substantial influence on both magnetic anisotropy and the coercivity field. A new type of overlayer-constrained magnetic domain wall, with easy tunable width, has been identified. In the case of X = Cr, Mo a formation of XCo alloy resulting in a decrease in thickness of the magnetically effective Co layer has been deduced. In the case of X = Mo, a preferential orientation of the domain structure has been observed and explained by an additional in-plane anisotropy.

Magnetic ordering of ferromagnetic ultrathin films is the object of intensive study. Magnetic reorientation phase transition (RPT) in ultrathin films has been one of the challenging topics of recent studies. Thickness dependent properties and modification of surface or interface film structure give tremendous opportunities for material engineering [1] unattainable in bulk material. Thickness-driven RPT was initially investigated in iron [2] and cobalt [3] films. In-plane magnetic anisotropy tailoring by submonolayer cover layers of Cu, Fe, Ag, O and CO have been reported for Co/Cu systems [4, 5]. The influence of various cover layers of Au, Cu, Pd, Pt, Ag, W on perpendicular magnetic anisotropy [6-10], as well as the strong increase of RPT thickness induced by carbon contamination [11] has been investigated in cobalt ultrathin films. The influence of substrate surface single-crystal polycrystal modulation on magnetic Ni film properties has been reported [12]. The results mentioned above have been obtained mainly by *in-situ* measurements, which have a limited technical potential for complex and complementary magnetic investigation. Special nanostructures prepared for *ex-situ* studies are the subject of the present work. The influence of both underlayer and overlayer structures on the magnetic properties of ultrathin cobalt was investigated.

The samples were grown in a molecular beam epitaxy system equipped with effusion cells and electron guns, operating in the low range of a 10^{10} Torr vacuum [13]. 10 mm × 10 mm polished sapphire Al_2O_3 (11-20) single crystal wafers were used as substrates. The (110) Mo buffer layer of 20 nm was grown at 1000°C. Then the following structure was grown (see Fig. 1): (i) the Au film generally starts at $y > 0$; (ii) the Co wedge changes thickness (d) along

the *x* axis; (iii) the thickness *h* of the metal X (Ag, Cr or Mo) wedge increases along the *y* axis; (iv) a 10 nm thick gold layer covers the whole sample. The presented results focus on the influence of: (i) the Ag and Cr overlayers and (ii) Mo – both the overlayer and underlayer – on cobalt properties.

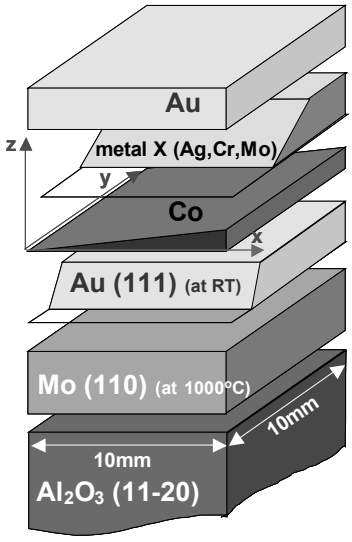

Fig. 1. Schematic view of samples

Ultrathin cobalt films were locally studied [14] using polar Kerr-effect-based techniques in (i) millimeter scale by a classic magnetooptical magnetometer – millimagnetometer; (ii) micrometer scale (by micromagnetometer) using an optical polarizing microscope with a cooled CCD camera system supported by image processing procedures. Magnetization distribution was investigated as a function of magnetic field $H_{\perp}$, $H_{//}$ applied perpendicular and/or parallel to the sample plane, respectively.

Let us first discuss the magnetic properties of Au/Co/Au films [14-16]. Figure 2A illustrates the sample remnant state – the image was calculated as a normalized differential image defined as $P(i,j) = (I_+(i,j) - I(i,j))/(I_+(i,j) + I(i,j))$, where I_+ and I denote images recorded after sample saturation by $H_{\perp} > 0$ and $H_{\perp} < 0$, respectively, and (i, j) denotes the position of a pixel along x and y directions, respectively. The gray level of the pixel is proportional to the local values of both the normalized remnant magnetization m_R and maximal Kerr rotation φ_{max}. By increasing silver overalyer thickness the transition between out-of-plane into an in-plane state occurs in the range of cobalt layer thickness between 1.3 nm and 1.8 nm.

The effective uniaxial anisotropy constant dependence on ultrathin film thickness d is usually described by the standard relation:

$$K_{1\text{eff}}(d) = 2\pi M_s^2 + K_{1v} + 2K_{1sm}/d \tag{1}$$

with contributions of volume K_{1v} and mean surface K_{1sm}, originating from the interfaces with buffer and overlayer. Combined studies [14], performed by the millimagnetometer and the

micromagnetometer, enabled determination of the following spatial distribution (see Fig. 2B) of magnetic anisotropy field $H_A = 2K_{1eff}/M_s$

$$H_A(x,y) = H_A^{Au}(x) + [H_A^{Ag}(x) - H_A^{Au}(x)] \times \left[1 - \exp\left(-\frac{h(y)}{h_A^*}\right)\right] \tag{2}$$

where H_A^{Au} , H_A^{Ag} are the anisotropy fields in Au/Co(d)/Au, Au/Co(d)/Ag(6 nm)/Au regions, respectively; h_A^* is the characteristic magnitude of exponential dependence and is equal to about 1 nm [14].

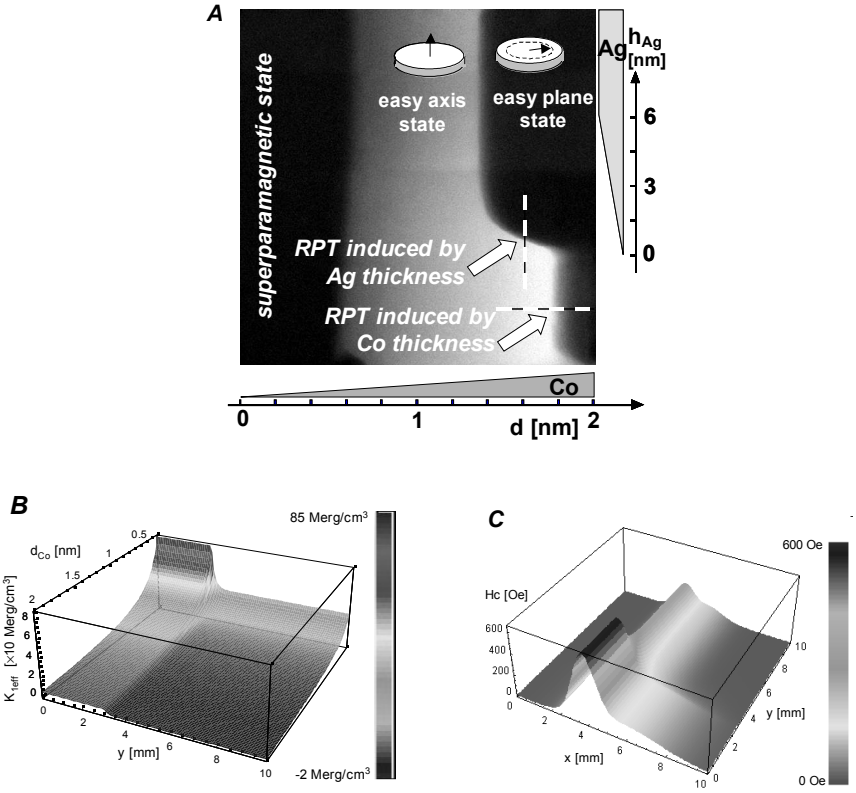

Fig. 2. Silver-induced tuning of magnetic properties: A) image of remnant state; B) spatial distribution of magnetic anisotropy; C) spatial distribution of coercive field

Spatial distribution of the coercivity field was determined [15] by analysing domain wall position during the magnetization reversal process, see Fig. 2C. This distribution could be described by

$$H_C(x,y) = H_C^{Au}(x) + \left[H_C^{Ag}(x) - H_C^{Au}(x)\right] \times \left[1 - \exp\left(-\frac{h(y)}{h_C^*}\right)\right] \tag{3}$$

where H_C^{Au}, H_C^{Ag} are the coercive fields in Au/Co(d)/Au, Au/Co(d)/Ag(6nm)/Au regions, respectively; h_C* is the characteristic magnitude of exponential dependence and is equal to 0.8 nm [15]. The magnetization reversal process is illustrated [16] in Fig. 3 where the sample was initially saturated by a magnetic field $H_\perp < 0$ in the "black" direction, then $H_\perp > 0$ was applied. Images were registered at $H_\perp = 0$. With the increasing reversal field amplitude, two "white" reversed areas expand from the sample low coercivity regions towards the high coercivity one. At the beginning of the reversal process (at low filed amplitude) the magnetization reversal process is dominated by a domain nucleation mechanism with a decreasing number of nucleation centers. As the domain wall propagates further upon the higher magnetic field, its structure becomes less complicated, taking an almost linear shape for d equal to about 1 nm. The wall position, shifted by H, is determined by coercivity field distribution. Finally, several additional nucleation centers appear again in the neighborhood of maximum H_C. A magnetic after-effect similar to the one reported in Refs [17, 18] was observed.

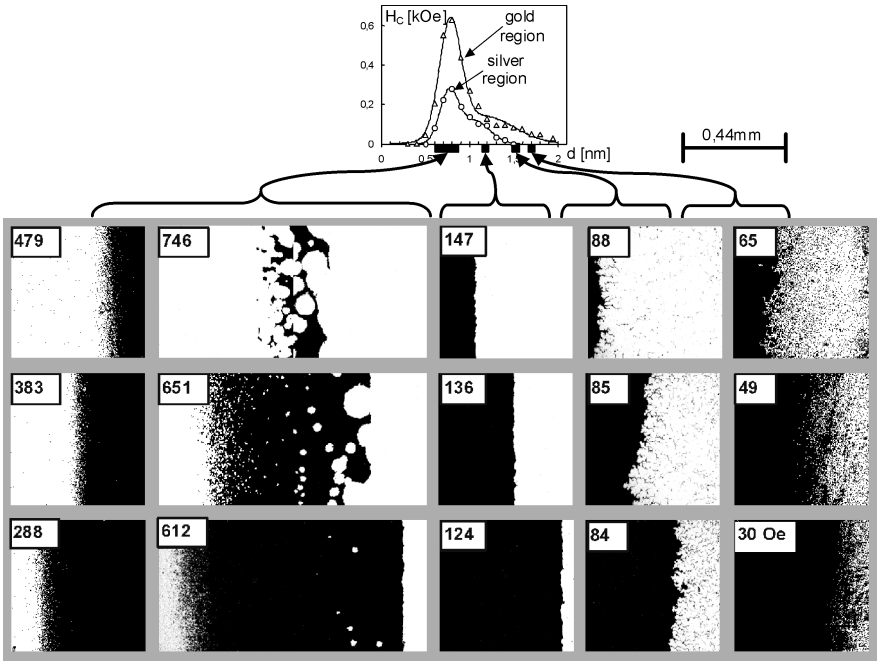

Fig. 3. Domain structure images registered in the "gold" region Au/Co(d)/Au for different d ranges (arranged in columns), marked as black squares in the inset showing the dependence of coercive field on thickness (for comparison the $H_C(d)$ dependences for Au/Co/Au and Au/Co/Ag are shown). Number in the left-upper corner of each image means the magnitude of magnetic field (in Oe), which have been applied during reversal process

Figure 4 shows the influence of the Cr overlayer [19] on magnetic properties of Co. The RPT is similar as the one discussed above for Co with Ag/Au overlayer. There is a curvature of the boundary limiting the left-hand-side dark area with zero remanence visible close to the left edge of the sample. The shape of this region could be explained by a formation of CrCo

alloy of about 0.17 nm in thickness resulting in a decrease in thickness of the magnetically effective Co layer. Such an effect was not observed for the Ag/Au overlayer because both Ag and Au have a sharp interface with Co.

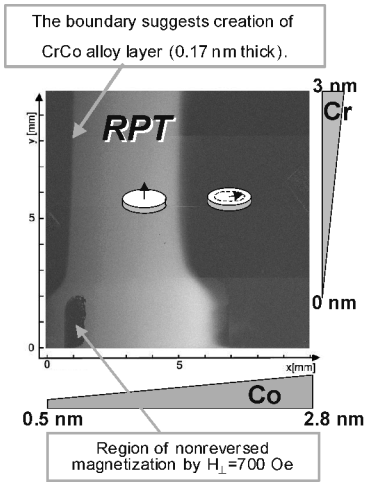

Fig. 4. Image of remnant state of the sample Au/Co/Cr-Au

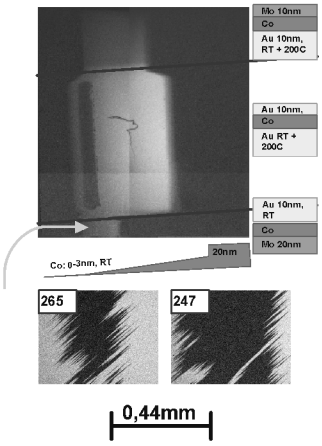

Fig. 5. Image of remnant states of the whole sample Au-Mo/Co/Mo-Au. The different areas of the sample are distinguished by straight black lines and are described by schematic diagrams. Two bottom images show domain structure registered at the point indicated by the arrow during reversal process after applying magnetic field with the magnitude displayed (in Oe) in the left-upper corner of each image

Three sample regions could be distinguished in Fig. 5: (i) Mo/Co/Au with Mo underlayer; (ii) Au/Co/Au – reference "gold" region ; (iii) Au/Co/Mo with Mo overlayer. Creation of the CoMo alloy, with similar thickness as discussed above for the CrCo one, can be deduced for the Au/Co/Mo region. Creation of the CoMo alloy is more evident in the Au/Co/Mo region than in Mo/Co/Au because of the much higher energy of Mo ions (during the deposition on Co) than Co ions (during the deposition on Mo). The domain structure shows a preferential orientation (about 45 degrees to Co thickness gradient) during magnetization reversal, see Fig. 5. This effect could be explained by the existence of additional in-plane anisotropy connected with a magnetoelastic contribution, similar to the one discussed for Co grown on *W* (110) [20]. It can be described by the following formula:

$$E_A = K_{1\text{eff}} \sin^2\theta + K_{\text{pl}} \sin^2\theta \cos^2\varphi \qquad (4)$$

where φ is measured from [001] Mo ([11-20] Co) and the in-plane axis is distinguished by the anisotropy term with K_{pl} constant.

The structure of both the underlayer and overlayer can be effectively used for the tuning of ultrathin magnetic film properties, such as magnetic anisotropy, the coercivity field and magneto-optical parameters. These possibilities seem to be important for general physics and application. Detailed theoretical description of these observed phenomena is an open problem.

Acknowledgements

This work was supported by the Polish State Committee for Scientific Research (grant No. 2P03B 065 15).

References

[1] B. Heinrich and J. A. C.Bland (Eds.), *Ultrathin Magnetic structures*, Springer, Berlin, 1994; and references therein.
[2] R. Allenspach and A. Bischof, Phys. Rev. Lett. **69**, 3385 (1992).
[3] M. Speckmann, H. P. Oepen and H. Ibach, Phys. Rev. Lett. **75**, 2035 (1995); H. Oepen *et al*., Phys. Rev. B **55**, 2751 (1997).
[4] W. Weber *et al*., Nature, (London) **374**, 788 (1995); W. Weber *et al*., Phys. Rev. Lett. **76**, 3424 (1996).
[5] S. Hope *et al*., Phys. Rev. Lett. **80**, 1750 (1998); J. A. C. Bland *et al*., J. Appl. Phys. **85**, 4613 (1999).
[6] P. Beauvillain *et al*., J. Appl. Phys. **76**, 6078 (1994).
[7] B. N.Engel *et al*., J. Appl. Phys. **75**, 6401 (1994).
[8] T. Duden and E. Bauer, Phys. Rev. B **59**, 468 (1999).
[9] K. Hyomi *et al*., Appl. Phys. Lett. **80**, 282 (2002).
[10] M. Dreyer *et al*., Phys. Rev. B **59**, 4273 (1999).
[11] J. Kim *et al*., Appl. Phys. Lett. **79**, 93 (2001).
[12] S. P. Li *et al*.**,** Phys. Rev. Lett. **88**, 87202 (2002).
[13] A. Wawro *et al*., Thin Solid Films **412**, 34 (2002).
[14] M. Kisielewski *et al*., Phys. Rev. Lett. **89**, 87203 (2002).
[15] M. Kisielewski *et al*., J. Appl. Phys. **93**, 7628 (2003).
[16] M. Kisielewski *et al*., physica status solidi (a) **196**, 129 (2003).
[17] J. Ferré *et al*., Phys. Rev. B **55**, 15 092 (1997).
[18] M. Kisielewski *et al*., J. Magn. Magn. Mater. **260**, 231 (2003).
[19] M. Kisielewski *et al*., J. Magn. Magn. Mater. **272-276**, e861 (2004).
[20] H. Fritzsche, J. Kohlhepp, and U. Gradmann, Phys. Rev. B **51**, 15933 (1995).